Journal of Statistical Physics, Vol. 110, Nos. 3–6, March 2003 (© 2003)

The Statistical Mechanics of Semiflexible Equilibrium Polymers

Apratim Chatterji[1,2] **and Rahul Pandit**[1,2]

Received April 29, 2002; accepted September 30, 2002

We give an overview of studies of models for semiflexible, equilibrium polymers with special emphasis on our work on both lattice and continuum models for such systems. We show, principally by Monte Carlo simulations, that, once monomers self assemble to form polymers, their semiflexibility leads to nematic phases at low temperatures. Attractive wall potentials encourage the adsorption of these equilibrium polymers on surfaces. Rapid cooling leads to the formation of glasses with entangled polymers. Shear promotes nematic ordering, but, at high shear rates, this tendency decreases since the equilibrium polymers are torn apart. A version of our model in which the polymers are directed shows the polymer analog of bosonic Mott-insulating, mass-density-wave, and supersolid phases. We give a brief comparison of our work with other studies and also explore the experimental implications of our study.

KEY WORDS: Semiflexible polymers; equilibrium polymers.

It is a great honor and pleasure to contribute this paper to the special issue of *Journal of Statistical Physics* for Professor Michael Fisher's seventieth birthday. He has influenced us all by the high intellectual standards that he has used in his work and which he has also demanded of others in the field of statistical mechanics. We look forward to his incisive comments and guidance and wish him many more years of active reaseach in this field.

[1] Centre for Condensed Matter Theory, Department of Physics, Indian Institute of Science, Bangalore 560 012, India; e-mail: rahul@physics.iisc.ernet.in

[2] Also at Jawaharlal Nehru Centre for Advanced Scientific Research, Bangalore, India.

0022-4715/03/0300-1219/0 © 2003 Plenum Publishing Corporation

1. INTRODUCTION

In systems of *equilibrium* polymers the lengths L of polymers fluctuate to yield a length distribution $P(L)$ that depends on the temperature T, the chemical potential μ, and other thermodynamic fields. These length fluctuations arise because polymer scission and fusion energies are comparable to k_BT, where T is the temperature and k_B is the Boltzman constant (henceforth we set $k_B = 1$). Some early papers[1] use the name *living* polymers, but the modern consensus is to reserve the term living for polymers in which monomers are only added to or removed from the ends of chains; in all other cases where polymer lengths fluctuate we use the term equilibrium polymers.

Experimental realizations of systems of equilibrium polymer abound.[2] They include wormlike micelles in water-surfactant mixtures[3] with surfactants like Cetyltrimethyl Ammonium Bromide (CTAB)[4] and 3-hydroxy-naphthalene-2-carboxylate, (SHNC)[5–8] or Cetyltrimethylammonium Tosilate (CTAT),[9, 10] liquid sulfur[11] and selenium, DNA molecules,[12] and poly (α-methylstyrene).[13–17] Some of these systems, like the micelle-forming water-CTAB-SHNC system, yield equilibrium polymers that are also semiflexible, i.e., there is a positive energy cost for bends in the polymers, so they form nematic phases at low temperatures.

There have been several experimental studies of the formation and behavior of living polymers[13–17] in dilute solutions of poly (α methylstyrene). The polymerization temperature T_p has been determined as a function of the initial mole fraction of monomers:[13] T_p depends strongly on the initial concentration of monomers but weakly on the nature of the solvent. In good solvents the degree of polymerization rises rapidly below T_p; this increase and the behavior of various thermodynamic functions in the vicinity of T_p have been fit to the predictions of a dilute $O(n)$ spin model in the limit $n \to 0$ in which there is an underlying continuous phase transition.[18, 19] Scattering studies[15] show that the mean radius of gyration of equilibrium polymers first rises, as the temperature is lowered below T_p, and then saturates as the polymers start overlapping. At this saturation metastability is observed, especially while heating the system. Furthermore, the pure liquid of monomers forms very viscous glassy systems of polymers with long equilibration times.[20]

Water-surfactant systems can form wormlike micelles which behave like equilibrium polymers. Dilute solutions of wormlike micelles have been studied.[21] The more concentrated systems studied subsequently showed evidence for semiflexibility. In particular, they showed interesting viscoelastic and relaxation properties and shear-induced nematic formation. Deuterium NMR spectroscopy in a Couette cell showed a shear-induced

isotropic to nematic transition in the concentrated wormlike-micelle system $CTAB/D_2O$.[22] Stress plateaux were seen in water-surfactant systems with wormlike micelles[23] and detailed studies of the relaxation behavior of shear stress, on the application of different shear fields, were also carried out.[24] Small-angle neutron-scattering studies[21] showed that the tumbling instability of nematic wormlike micelles results in oscillations in shear-stress responses. Representative rheological investigations of such wormlike micellar systems include refs. 9, 10, and 25; these showed, *inter alia*, that the the measured stress was a nonmonotonic function of the shear rate $\dot{\gamma}$;[9, 10] in other experiments, where the stress was controlled externally, the stress-strain curves showed a plateau for $\dot{\gamma}$ larger than some critical strain rate.

The development of a theoretical understanding of the experiments described briefly above is an important challenge in the statistical mechanics of complex fluids. Several models have been developed for this purpose and considerable progress can be made by semi-analytical methods in the dilute case. In particular, there is reasonable agreement between experiments, simulations, and theory[26] on the form of the length distribution $P(L)$ of the lengths L of equilibrium polymers in such dilute systems.[26–29] A simple minimization of a Flory–Huggins-type free energy with Gaussian chains with a finite scission and fusion energy yields an exponential length distribution in the semidilute case;[26, 29] in the dilute case the distribution crosses over to the Schulz–Zimm form.[29]

Approximate, mean-field methods for the study of phase transitions from isotropic to nematic or hexagonal-columnar phases in more dense systems have also been developed[30, 31] by using phenomenological free energies. We concentrate on complementary studies[32–37] that have used numerical simulations to obtain a detailed understanding of the statistical mechanics of models for semiflexible, equilibrium polymers in systems that are dense enough to form mesophases at low temperatures.

Given the complexity of the statistical mechanics of semiflexible equilibrium polymeric melts, early studies were restricted to lattice models. In very special limits, these models can be studied analytically; however, for generic parameter values computer-simulation methods have to be used. Most studies concentrated on *either* semiflexible *or* equilibrium polymers;[29, 38–40] a few, however, studied lattice models in which equilibrium polymers, once formed, were semiflexible.[41–45] Lattice models suffer, perforce, from a variety of artifacts, so the next natural step was to develop continuum or off-lattice models for polymers. This was done by a few groups[32, 34–37, 46–51] over the past decade or so since the improvement of computational facilities made it possible to study the statistical mechanics of such off-lattice models by computer-simulation methods.

To the best of our knowledge, ours is the only off-lattice model for equilibrium polymers which, when formed, are also semiflexible;[32] other models described *either* semiflexible *or* equilibrium polymers. Our study covers both *equilibrium* phenomena, such as phase diagrams and thermodynamic functions in the vicinity of the isotropic-nematic transition, and *nonequilibrium* ones, like glass formation and the response of our model system of semiflexible, equilibrium polymers to shear. We caution the reader that the name "equilibrium polymers" does *not* mean that we restrict our work to studies of the equilibrium statistical mechanics of these systems. In Section 2 we give a brief overview of models for semiflexible, equilibrium polymers with special emphasis on the ones developed in our group;[32, 43–45] we end this section with a summary of our principal results. Section 3 is devoted to details of our calculations and results. Section 4 contains concluding remarks.

2. LATTICE AND OFF-LATTICE MODELS

2.1. Overview of Models and Studies of Equilibrium and Semiflexible Polymers

Early work[18] which suggested that reversible polymerization could be treated as a phase transition was shown[19] to be equivalent to a mean-field treatment of a model for a magnetic phase transition in an n-component $O(n)$ model in the limit $n \to 0$. These studies have been extended to a dilute $O(n)$ model again in the limit $n \to 0$[52–54] and compared in detail with experiments[13–15] on dilute solutions of poly (α methylstyrene). (If ring polymers are allowed,[55] one must use $n = 1$.) Metastability effects manifest themselves as the solution becomes concentrated; and our emphasis in this paper is on systems that are concentrated enough either to yield liquid-crystalline mesophases or metastable states.

The bond-fluctuation model[38] has also been successful in describing the static and dynamic properties of equilibrium polymers. Though developed on a lattice, this model allows for fluctuating bond lengths and shows Rouse behavior for all dimensions. Static properties of equilibrium polymers have been studied using this model and have confirmed the crossover from Schulz–Zimm to exponential distributions as the system moves from the dilute to the semidilute cases[29] mentioned above. A Monte Carlo study of diffusion in a bond-fluctuation model with equilibrium polymers[40] has shown Rouse behavior.

Lattice-model studies that concentrate on the semiflexibility of polymers owe much to the early work of Flory[56] in which he developed a model for semiflexible (but *not equilibrium*) polymers on a lattice; the

polymers were modelled as self-avoiding random walks on a three-dimensional lattice and an energy penalty was introduced for right-angle bends. Flory's mean-field treatment of this model yielded a first-order phase transition from an isotropic phase, in which the polymers had a high density of bends, to an ordered state in which the polymers pointed, on average, along one of the axes (x, y, or z) of the lattice; this ordered phase could either be thought of as an orientationally ordered polymer nematic or a polymer crystal because of the underlying periodicity of the lattice (this is a lattice-model artifact that subsequent off-lattice studies have overcome). Monte Carlo simulations[57] corroborated and developed Flory's results; however, there was some controversy about the nature of the transition especially in a two-dimensional version of the Flory model. For a recent discussion of this issue see ref. 45, which explains why the two-dimensional case is subtle: in essence this is because, in an enlarged parameter space, Flory's model lies close to the F model, which displays a high-temperature phase with algebraically decaying correlations.

Lattice models for semiflexible equilibrium polymers have generalized Flory's model by introducing energies for open ends, etc., as we describe below.[43–45] In addition there has been another class of lattice models which we term independent-monomer-state (IMS) models[45] in which truncated link configurations at vertices attach to form polymers.[41, 42] These models also describe semiflexible, equilibrium polymers; their phase diagrams have been studied in detail and show a transition from a disordered state to one with aligned polymers; this transition can be second-order or first-order, with a tricritical point in between.[41, 42] However, these IMS models admit configurations not present in the types of lattice models we study below, in which monomers occupy the links of the lattice.[45]

To overcome the constraints of lattice models, off-lattice studies of fixed-length polymers have been proposed; these often use bead-spring-type models.[35, 46] They have been used to study dilute and concentrated polymers solutions. In addition to static properties like chain radii, internal energy and specific heat, dynamical properties like mean-square displacements, relaxation times and diffusion constants have also been obtained.[35] In another study, this model has been used to study polymers in random media.[46] The influence of the degree of semiflexibility on the isotropic-nematic phase transition has been studied,[49] as a function of density of monomers for polymers of fixed length, by using a free-energy minimization techniques. Further studies of systems of semiflexible polymers have used molecular-dynamics simulation and the finitely extendable nonlinear elastic (FENE) potential;[47] by using partially stiff and fully stiff fixed-length polymers, this study finds solid, smectic, and liquid phases but no nematic phase. This FENE model has also been modified suitably to yield

equilibrium polymers[36] and used, in the dilute and semidilute regimes, to study the behavior of equilibrium polymers under shear flow: It is found that individual conformations of chains tend to elongate along the flow direction, the mean polymer length decreases as the shear rate increases, and that the molecular-weight distribution changes from the power-exponential Schwartz form to a mean-field-type exponential distribution function at high shear rates. Our off-lattice model[32] in which monomers self assemble to form semiflexible, equilibrium polymers is described in detail below.

We summarize first the essential qualitative results that follow from the studies of the lattice[43–45] and continuum models[32] developed in our group. At high temperatures T all these models have a disordered phase in which there are short polymer chains with a large number of bends. The length distribution $P(L)$ of polymer chains drops exponentially with L. As T is lowered, phase transitions occur yielding an ordered phase with long, predominantly aligned polymer chains and a low density of bends. The precise nature of the transition depends on the dimension d; e.g., if $d = 2$ the transition is continuous and in the universality class of the two-dimensional, Ising-model transition for the model of refs. 43–45; however, if $d = 3$ the transition is first-order. In lattice models the low-temperature ordered phase can be interpreted as a polymer crystal; but, in continuum models such as that of ref. 32, it is a polymer nematic. Thermodynamic functions such as the density and the nematic order parameter show a jump at this transition.

We have also studied adsorption at neutral and attractive walls in our continuum model. We find, in particular, adsorbed films on attractive walls, as we approach the bulk isotropic-nematic phase boundary. These adsorbed layers show enhanced nematic ordering relative to the bulk.

We have studied the effects of shear in our continuum model by a dynamic Monte Carlo method (Section 3). We observe that shear promotes nematic alignment in our system of equilibrium polymers at low shear rates. However, at high shear rates the chains get torn apart so this nematic ordering decreases. This tearing apart has been noted in earlier studies of equilibrium polymers that are not semiflexible.[47]

Equilibration is very slow in both lattice and continuum models especially at low temperatures: the mean polymer length $\langle L \rangle$ is large, so glasses form easily. In particular, if we quench our system from high to low temperatures, we get disordered, metastable states that are glass-like as we show explicitly by a Monte-Carlo analog of scanning calorimetry. We also present some differential scanning calorimetry results which are consistent with experimental results on the glass formation temperature. The effect of bounding walls on glass formation temperature is also investigated.

2.2. Our Models

2.2.1. Lattice Models for Semiflexible Equilibrium Polymers

Lattice models for semiflexible polymers date back at least as far as the seminal work of Flory[56] mentioned above. Models for equilibrium polymers allow the lengths of such polymers to fluctuate by including an energy cost for the scission of polymer chains and for their open ends. Early studies of systems of equilibrium polymers[41, 58] concentrated on the statistics of completely flexible ($\varepsilon = 0$) polymer chains. Subsequent studies have included both scission and fusion of polymer chains along with semiflexibility. We illustrate this for the lattice model of refs. 43–45 in which the variables occupy the links of a d-dimensional hypercubic lattice and assume the value 0, if no monomer is present, and 1, if a monomer is present; at most one monomer is allowed per link, i.e., polymers avoid each other and themselves. For example, for $d = 2$ we have a square lattice in which it is convenient to associate two links with every site (i, j) and use the link variables $n_x(i, j)$ and $n_y(i, j)$ that occupy, respectively, the left $(-x)$ and the downward $(-y)$ links emanating from it. Monomers can fuse to form polymers. Semiflexibility is introduced via a positive energy cost ε for right-angled bends, there is a chemical potential μ for vacancies (i.e., sites which have no monomers on *all* emanating links), and an energy $h > 0$

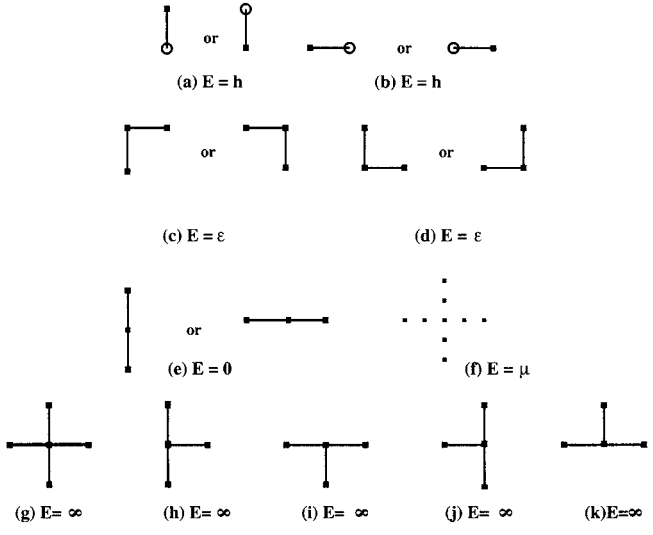

Fig. 1. Link configurations and corresponding energy costs E in the model of refs. 43, 44, and 45. Full lines indicate links occupied by monomers, whereas dashed or blank ones show unoccupied links. There is an energy cost h for open ends, ε for bends, and μ for vacancies. Branching is disallowed by virtue of infinite energy costs for trivalent and tetravalent vertices.

for open ends; branching of equilibrium polymers is forbidden in this model but the formation of ring polymers is allowed. (For $d = 2$ see Fig. 1.) For $d = 3$ it is useful to introduce a mild attractive energy cost between monomers on parallel links of a plaquette. This disfavors the formation of ground states in which the polymers in a plane are aligned but successive planes are stacked randomly.[45]

2.2.2. Directed Semiflexible Equilibrium Polymers

We have recently modified[33] the lattice model described above so that the polymers, once formed, are directed, on average, along a given direction. This model for *directed, semiflexible, equilibrium* polymers is of relevance in studies of vacancy and interstitial strings in columnar phases in discotic liquid crystals.[59] Figure 2 shows the energies of different link configurations in this model for $d = 2$. Note, in particular, the negative energy γ that promotes the formation of equilibrium polymers directed

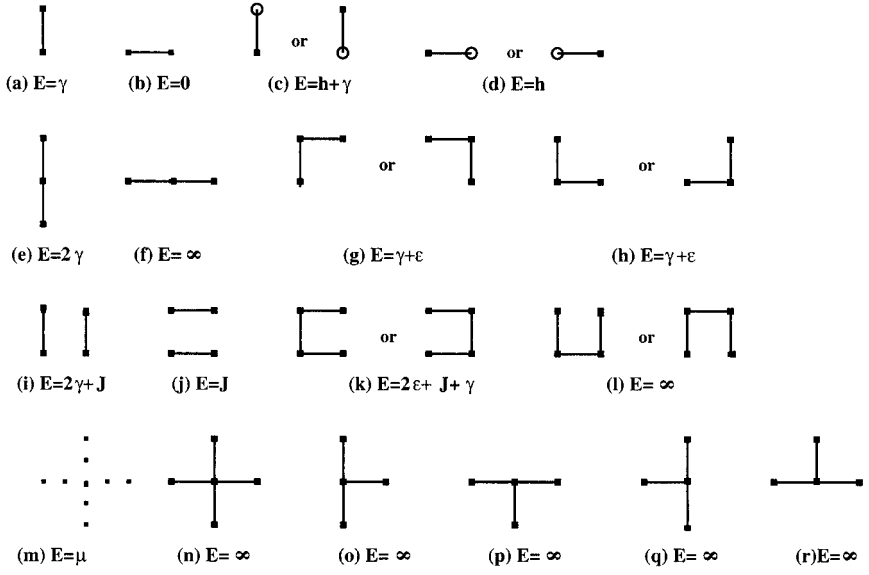

Fig. 2. Link configurations and corresponding energy costs in our model for directed semiflexible polymers. Full lines indicate links occupied by monomers, whereas dashed or blank ones show unoccupied links. Infinite energy costs indicate disallowed configurations. ε is the energy for bends and can be greater than, equal to, or less than 0; $h > 0$ is the energy for open ends; $\gamma < 0$ favors links in the y direction; μ is the chemical potential for vacancies; $J > 0$ is the repulsive energy cost for occupied parallel links on opposite side of a square plaquette. Branching, hairpin bends along the y direction, and two consecutively occupied x links are forbidden. (In the studies we present here $\mu = 0$.)

preferentially along the vertical (y) axis. Hairpin bends along the y direction and 2 or more consecutive occupied links in the x direction are forbidden. We also introduce a mild, repulsive energy cost $J > 0$ between monomers on parallel links of a plaquette. To examine the competition between phases in which the polymers, once formed, straighten and those in which they meander and wind around the system we have studied our directed model for (a) $\varepsilon > 0$, (b) $\varepsilon < 0$, and (c) $\varepsilon = 0$. At low temperatures, the polymers formed prefer to be straight in case (a) whereas in cases (b) and (c) the polymers wind around the lattice with a high density of bends.

For case (c), i.e., flexible polymers with $\varepsilon = 0$, this model can be mapped on to a model of hard-core bosons on a lattice with an extended-Hubbard-type repulsion between bosons on nearest-neighbor sites.[60–62] The polymers can be visualised as the world lines of these bosons.[61, 62] Since 2 or more consecutive occupied links in the x direction are forbidden in our directed-polymer model, its bosonic analog allows only for hopping between nearest-neighbor sites. The square of the winding number of the polymers can be shown to be proportional to the superfluid density of bosons.[63–65]

2.2.3. Continuum Models

Lattice models of the type discussed above have the virtue that they can be studied in great detail by say Monte Carlo simulations. However, the underlying lattice introduces certain artifacts which can be overcome only by using continuum or off-lattice models. For example, it is not straightforward to distinguish between nematically ordered polymeric phases and a crystalline stacking of polymers in a lattice model because of the periodicity imposed by the lattice. Most off-lattice models for equilibrium polymers use the bead-spring or FENE models mentioned above. These have concentrated either on equilibrium polymers that are not semiflexible or on semiflexible polymers that are of fixed length. A notable exception is the work of refs. 30 and 31 which has studied the formation of nematic and hexagonal phases in systems of wormlike micelles by using an approximate mean-field theory with a phenomenological free energy.

The goal of our recent work has been to develop an off-lattice molecular model for self-assembling, semiflexible, equilibrium polymers and study its statistical mechanics by Monte Carlo (MC) simulations. Our model accounts for such semiflexibility by using an *isotropic* two-body interaction $V_2(r)$ between monomers; the tendency to form linear, semiflexible chains without branches is brought in via a three-body interaction $V_3(r_{ij}, r_{ik}, \theta)$. These interaction potentials are given below:

$$V_2(r) = \epsilon[(2\sigma/r)^{12} - (2\sigma/r)^6] + \epsilon_1 \exp(-a(r/2\sigma)) - V_0, \tag{1}$$

with r the separation between two monomers, $\epsilon_1/\epsilon = 1.34$, $\sigma = 1$, $a = 1.72$, and V_0 such that the potential is continuous at the distance $r_{\max}$ beyond which we set $V_2(r) = 0$. We use $r_{\max}/\sigma = 5$, so $V_0/\epsilon = 0.0142$.

$$V_3(r_{12}, r_{13}, \theta) = \epsilon_3 \left(\frac{\sigma_3}{r_{12}} - 1\right)\left(\frac{\sigma_3}{r_{13}} - 1\right) \tan^2 \theta, \tag{2}$$

where $r_{ij} \equiv |\vec{r}_{ij}|$ and $r_{ik} \equiv |\vec{r}_{ik}|$ are, respectively, the separations of particles j and k from particle i, θ is the angle between $\vec{r}_{ij}$ and $\vec{r}_{ik}$, $\sigma_3/\sigma = 3$, and $\epsilon/\epsilon_3 = 4.66$. For some of our studies we have also used a higher value of ϵ_3, namely $\epsilon/\epsilon_3 = 1.4$. We set $V_3(r_{12}, r_{13}, \theta) = 0$ if either $r_{12} > \sigma_3$ or $r_{13} > \sigma_3$. A representative plot of our potential is given in Fig. 3. It is also useful to introduce a field that favors the formation of a nematic phase. We accomplish this by assigning an energy $-H_n^2 \cos^2 \phi$ for a segment of polymer chain connecting nearest-neighbor monomers, with ϕ the angle between the z axis and the vector connecting one monomer to its nearest neighbor.

At large distances the two-body potential V_2 goes from being attractive to repulsive at $r \simeq 3\sigma$. Thus we use the convention that, if the distance between two monomers is $\leqslant 3\sigma$ at a given instant, then they belong to the same polymer at that time. Of course the assignment of monomers to polymers changes with time in our model for equilibrium polymers. Our qualitative results do not depend upon this convention. Similarly we expect the qualitative aspects of our study (as opposed to quantitative results for transition temperatures, etc.) to be independent of the specific parametrization we use for V_2 and V_3, which is a convenient way of building in the following physical requirements: Monomers should aggregate to yield semiflexible, equilibrium polymers that do not branch; and different strands of well-formed polymers should avoid each other. Branching is avoided by a combination of self avoidance constraints and the high energy

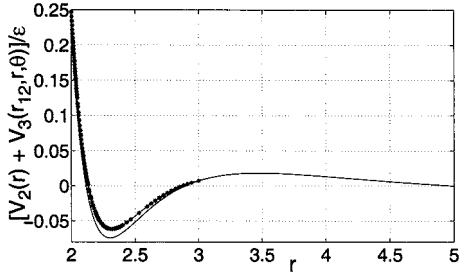

Fig. 3. Representative plot of the potential $[V_2(r)+V_3(r_{12}, r_{13}, \theta)]/\epsilon$ used in our off-lattice model for $\theta = 0$ (full line), and $\theta = 45°$ (line with *), $r_{12} = 2.5\sigma$, and $r_{13} = r$. $V_3(r_{12}, r, \theta) = 0$ for $r > 3\sigma$; and $V_2(r) = 0$ for $r > 5\sigma$ (we use units with $\sigma = 1$).

of right angled bends because of the $\tan^2\theta$ term in the potential V_3. The specific microscopic potentials that lead to such equilibrium polymers will of course depend on the particular physical system being considered; and those appropriate for the formation of wormlike micelles in water-CTAB-SHNC mixtures, will be quite different from the V_2 and V_3 we use.

To study the adsorption of the equilibrium polymers on surfaces we introduce two bounding walls perpendicular to the x direction at $x = 0$ and $x = 300\sigma$; in the y and z directions we use periodic boundary conditions. Furthermore we assume that the monomers interact with the walls via the potential[68]

$$V_w = w[(2\sigma_w/x)^9 - (15/2)(2\sigma_w/x)^3], \tag{3}$$

which is attractive at long distances; the parameter w specifies the strength of V_w and σ_w governs the position of its minimum; and x is the distance from the nearest wall to the monomer in question.[67, 68] For convenience we have used $\sigma_w = \sigma = 1$ and $w/\epsilon = 14.286 \times 10^{-4}$ for attractive walls; for neutral walls we use $w/\epsilon = 14.286 \times 10^{-8}$. In our simulations we use the form of V_w in Eq. (3) for $x < 7\sigma_w$; for $x > 7\sigma_w$ we set $V_w = 0$ and to ensure continuity of the potential at $x = \sigma_w$ we add a suitable constant to V_w. Specifically, for $x < 7\sigma_w$ we use $V_w = w[((2\sigma_w/x)^9 - (15/2)(2\sigma_w/x)^3 + 0.1749]$.

3. CALCULATIONS AND RESULTS

3.1. Calculations

3.1.1. Semiflexible Equilibrium Polymers: Lattice Model

Given the complexity of the models that we have described above, it is not possible to study their statistical mechanics by analytical methods. However, there are a few special limits in which our lattice model can be mapped on to an exactly solvable vertex model. Both our lattice models map on to 11-vertex models if we use a two-dimensional, square lattice. If we forbid vacancies and open ends, by assigning infinite energy costs to them, the simple lattice model described above maps on to an F model which can be solved exactly;[66] at certain specific values of the temperature this model can be mapped on to a free-fermion model.[45] In the general case, however, this model must be studied by computer-simulation methods. As described in ref. 45, the Monte Carlo algorithm of Metropolis *et al.* is used in conjunction with single-link updates and, where necessary, multiple-link updates to facilitate equilibration at low T. Since we are studying a model of equilibrium polymers it is natural to use the grand-canonical ensemble.

3.1.2. Directed Semiflexible Equilibrium Polymers

We study our model for directed semiflexible equilibrium polymer by a straightforward extension of the Monte Carlo method used in ref. 45. In particular, we use the grand-canonical ensemble with single-links updates.[33] We concentrate here on the directed-polymer analogs of superfluid phases in bosonic models and restrict our study to two dimensions. Since the polymers are directed along the y direction, we use lattices of size $L_x = 12$ and $L_y = 60$ for all the results reported here. We have checked, though, that larger lattices give the same results. We have studied this model for $\varepsilon > 0$, $\varepsilon = 0$, and $\varepsilon < 0$, and also for various values of h and J (see Fig. 2). Here we give representative data only for $\varepsilon = 0$ and $\varepsilon = 1$ with $h = 8$ and $J = 1$ and refer the reader to ref. 33 for a systematic study of this model. We have calculated, as a function of the temperature T, the internal energy U, the specific heat C, the square of the winding number $\langle W^2 \rangle$, which characterizes superfluid ordering for $\varepsilon \leqslant 0$, and the mass-density-wave (MDW) order parameter for $\varepsilon = 1$. The MDW order parameter m_{MDW} is defined as follows:

$$m_{\mathrm{MDW}} = \sum_{j=1}^{L_y} \sum_{i=1}^{L_x} (-1)^i \, (2n_y(i, j) - 1)/M, \tag{4}$$

where M is the total number of links. To calculate winding numbers we follow Monte Carlo simulations of bosonic models[63, 64] in which the boson world lines are like our directed polymers. The superfluid density ρ_s and the winding number are related via $\langle W^2 \rangle = 2\rho_s(T)\, \hbar^2 / m k_B T$.[63–65]

We start our simulations at high temperatures and then cool our system slowly to reach the ordered state. At each value of temperature, we allow our system to equilibrate for 3×10^5 MCS, after which we collect data to for thermodynamic averaging every 50 iterations for 10^5 MCS. We then heat our system by using the configuration at the lowest temperature reached as the initial configuration for the heating run. Metastable states hamper equilibration especially for $\varepsilon = 0$ and at low T; these are especially pronounced for $\langle W^2 \rangle$.

3.1.3. Continuum Models

As in our lattice models, we use the grand-canonical ensemble in the Monte Carlo simulations of our off-lattice model of equilibrium polymers; thus we introduce a chemical potential μ for monomers. [For the sake of notational conformity with our earlier studies,[32, 43–45] we use the symbol μ to denote the chemical potential for vacancies in our lattice models; but it denotes the chemical potential for monomers in our off-lattice model. We hope the meaning of the symbol μ will be clear from the context in which it

is used.] Thus the isotropic-nematic phase boundary is a line in the μ–T plane. We use the canonical ensemble only in those simulations where we investigate the effect of shear on the system. We use periodic boundary conditions and a cubical box of side $\ell = 60\sigma$ for most of our studies. We have also checked that our results remain qualitatively unchanged for larger system sizes, i.e., a cubical box of side $\ell = 78\sigma$. However, while studying adsorption at surfaces or the effect of shear on the system, we impose two bounding walls perpendicular to the x direction and use periodic boundary conditions along the two remaining directions.

For our studies of equilibrium phase diagrams, we start by placing 1000 monomers on a simple-cubic lattice inside the simulation domain. The positions of the monomers are then updated by using the algorithm of Metropolis, *et al.* The monomers self assemble to form polydisperse polymer chains with a length distribution $P(L)$ that depends on T and μ. We make 500–1000 attempts both to introduce and remove particles with suitable Boltzmann weights every 15 Monte Carlo steps (MCS). We equilibrate our system at a high temperature and gradually cool it by changing T/ϵ in steps of 7.14×10^{-5} till we reach the low-temperature nematic phase. We then take the configuration at the lowest temperature reached as the initial configuration and slowly heat our system till we reach the isotropic phase. At each temperature we allow the system to equilibrate for 30000 MCS after which we collect data for averages every 15 MCS for 60000 MCS to calculate thermodynamic functions. We calculate the internal energy U, the nematic order parameter $s = \langle (3\cos^2(\theta) - 1)/2 \rangle$, the average length of polymers $\langle L \rangle$, the mean number N of monomers in the box, the distribution of polymer lengths $P(L)$, and the aspect ratio A of polymer chains with more than 3 monomers. The angle θ required for the nematic order parameter is calculated by first distinguishing each chain, then calculating the moment-of-inertia tensor for each chain, diagonalizing this tensor, and finally obtaining the angle that the major axis makes with the nematic direction (in this case the z direction). The aspect ratio is measured by taking the ratio of the major axis and the minor axis. When we study our system in a larger box, i.e., when the box size is $\ell = 78\sigma$, we equilibrate over 45000 MCS and average thermodynamic functions over next 90000 MCS at each temperature.

To study the adsorption of polymers on walls, we introduced two bounding walls perpendicular to the x direction. Periodic boundary conditions are imposed along the other two directions. For the case of attractive walls we use the potential V_w as mentioned in Eq. (3); for the case of neutral walls, we reduce the strength of the attractive part of V_w but retain its repulsive part and use a system of size $300\sigma \times 60\sigma \times 60\sigma$. We calculate the layer density $\rho(x)$, at representative values of μ and T on the isotropic

side of the bulk isotropic-nematic phase boundary, by averaging over layers parallel to the walls; the thickness of each layer is taken to be σ. At each value of μ and T we equilibrate over 10^4 MCS and then collect data to calculate thermodynamic functions every 10 MCS for another 10^4 MCS. We make 3000 attempts to introduce and remove particles with suitable Boltzmann weights every 10 MCS. As we will discuss below, our data are good enough to show, pictorially, the adsorption of self-assembled polymers on attractive walls; however, our runs are not long enough to obtain complete surface phase diagrams which should show wetting transitions in these systems.[67, 68]

We impose shear on our system of equilibrium polymers by the dynamical Monte Carlo method.[36, 37] We apply an external field $F_z(x)$ along the z direction and let its magnitude change linearly along the x direction. We impose rigid walls perpendicular to the x direction and periodic boundary conditions along other directions. Specifically, we use

$$F_z(x) = \mathscr{B}(x/\ell - 1/2), \tag{5}$$

where $\mathscr{B}$ is a measure of the strength of shear whose magnitude is high near the walls and reverses direction in the middle of the box. To specify the shear in dimensionless units, we define $B \equiv \mathscr{B}\,\delta z_{\max}/\epsilon$, where $\delta z_{\max}$ is the maximum allowed value of δz in a single Monte Carlo move. When the position of a monomer is updated in a Monte Carlo move, then the work done by this applied field is also added to δE_1, the change in energy when the monomer changes its position from (x_1, y_1, z_1) to (x_2, y_2, z_2). Thus the total energy change δE used in our Monte Carlo update is

$$\delta E = \delta z\, \mathscr{B}\left(\frac{x_1 + x_2}{2\ell} - \frac{1}{2}\right) + \delta E_1. \tag{6}$$

We start our runs with 2700 monomers arranged in a simple-cubic lattice and work in the canonical ensemble, set $H_n/\sqrt{\epsilon} = 0$, and $\ell = 60\sigma$. We start at high temperatures and cool our system; we then start with the lowest-temperature configuration as the intial configuration for the heating run. In these runs the temperatute T is changed in steps of $\Delta T/\epsilon = 7.14 \times 10^{-5}$ and data are collected for averages every 30 MCS for 30000 MCS after initial transients are discarded for 15000 MCS.

To explore glassy states in our models we carry out Monte Carlo analogs of scanning-calorimetry studies. These were first used in our lattice-model[44, 45] studies. Here we present them only for our off-lattice model. As we illustrate below, a numerical derivative of our scanning-calorimetry plots of internal energy U/ϵ versus T/ϵ yields a conventional differential-

scanning-calorimetry (DSC) plot. We obtain glassy states by quenching our system rapidly from high T and cooling it by reducing T/ϵ in steps of 7.14×10^{-5} and holding it fixed at every stage for 300 MCS.

The energy U/ϵ for this cooling run is averaged over 150 MCS with data collected every 15 MCS. The disordered polymer state that obtains is then heated slowly in steps of 7.14×10^{-5}; at each stage in the heating run the system is allowed to relax for 15000 MCS and data for thermodynamic functions are collected every 15 MCS for another 30000 MCS. Furthermore, 1000 attempts are made to introduce or remove particles every 15 MCS. DSC experiments measure the "specific heat" C (strictly dU/dT). The specific heat shows a minimum at the temperature where the glass changes to the low-T equilibrium phase (nematic in our case). A subsequent peak indicates the change from the low-T equilibrium to the high-T (isotropic) phase. To make contact with experiments, we plot C (i.e., dU/dT) versus T. To obtain dU/dT we fit our plot of U/ϵ versus T/ϵ for the heating run with a 9th-order polynomial and take the derivative of this polynomial with respect to T.

Walls affect the glass-forming tendencies of polymeric systems.[70] Thus we have obtained the effect of attractive and neutral walls on our DSC studies. We find that the nature of the wall affects the temperature associated with the glass-nematic transition at which dU/dT shows a minimum. We use three wall separations, namely, 18σ, 36σ, and 72σ and periodic boundary conditions in the remaining directions with a box size of 60σ. For these three cases we start with 800, 1920, and 3800 monomers, respectively, and every 10 MCS we attempt to remove or add 200, 400, and 800 monomers, respectively, to the system. For the rapid-cooling run, data are collected over 100 iterations every 10 MCS at every value of T. Data for heating runs are averaged over 10000 MCS, and collected every 10 MCS; the value of $H_n/\sqrt{\epsilon}$ is 0.0207. The heating run starts at a temperature much higher than in the case without walls because the strongly attractive walls change the transition temperature, since we are now considering systems in which the walls are very close together. Of course, if the walls were infinitely far apart, they would not affect the bulk transition temperature.

3.2. Results

3.2.1. Semiflexible Equilibrium Polymers: Lattice Models

The lattice model of refs. 43–45 has been studied in both two and three dimensions. We only give a brief outline of the principal results here. At low temperatures there is a crystallization transition of polymers, provided

the system is cooled slowly enough to prevent glass formation. The phase transition is continuous in $d = 2$ and there is a first-order phase transition from the disordered phase to the crystalline phase at $d = 3$. These transitions can be characterized by the measurement of various thermodynamic functions. The relaxation of glassy metastable polymeric systems is very slow. Scanning calorimetry studies have been carried out and the results are qualitatively similar to those we report below for our off-lattice model. If the system is quenched rapidly to low T from high T, disordered metastable states are obtained. In three dimensions the glasses formed are completely disordered for high values of open-end cost h, but partially ordered lamellar glasses for intermediate values of h; relaxation out of glassy states is logarithmically slow for high h. Lowering h eases the frustration in disordered polymer networks, obtained on quenching, thereby inducing an apparently continuous glass transition, but this is not related to an equlibrium phase transition. This model has the obvious lattice artifacts mentioned above; the lamellar glass in this model is also a lattice artifact.

3.2.2. Directed Semiflexible Equilibrium Polymers

Qualitatively new phases arise if the equilibrium polymers in our lattice model are directed. In particular, we obtain polymer analogs of superfluid and mass-density-wave phases in lattice models for interacting bosons.

At high T we get short, disordered chains with a low value of the average length $\langle L \rangle$ for all values of ε. However, as the temperature is lowered, we get longer chains of self-assembled polymers. Their interactions then lead to the polymer analogs of a mass-density wave in the boson language, for $\varepsilon > 0$, and a superfluid phase with winding polymers for $\varepsilon \leqslant 0$. The top panel of Fig. 4 shows representative configurations for $\varepsilon = 0$ and $\varepsilon = 1$ respectively. If $\varepsilon \leqslant 0$ the polymers wind in our lattice. However, the mutual repulsion J between monomers and the self-avoidance constraints ensure that only every alternate site is occupied by a monomer; to this extent there is also mass-density-wave order in the system for $\varepsilon \leqslant 0$ and is reminiscent of a supersolid phase. Conventional mass-density-order shows clearly in the configuration of polymers for $\varepsilon = 1$, since there is only one aligned polymer on every other column (i.e., one boson at every other site). Plots of the specific heat C, $\langle W^2 \rangle$ and m_{MDW} versus T are also given in Fig. 4 for the above mentioned values of ε. The mass-density-wave order parameter m_{MDW} for $\varepsilon = 1$ shows a clear jump indicating a first-order transition. The shape of the specific heat plot suggests a more subtle KDP type transition,[33] though we have not been able to map our model on to an ice model.[66] The plots of C and $\langle W^2 \rangle$ versus T for $\varepsilon = 0$ are consistent with a

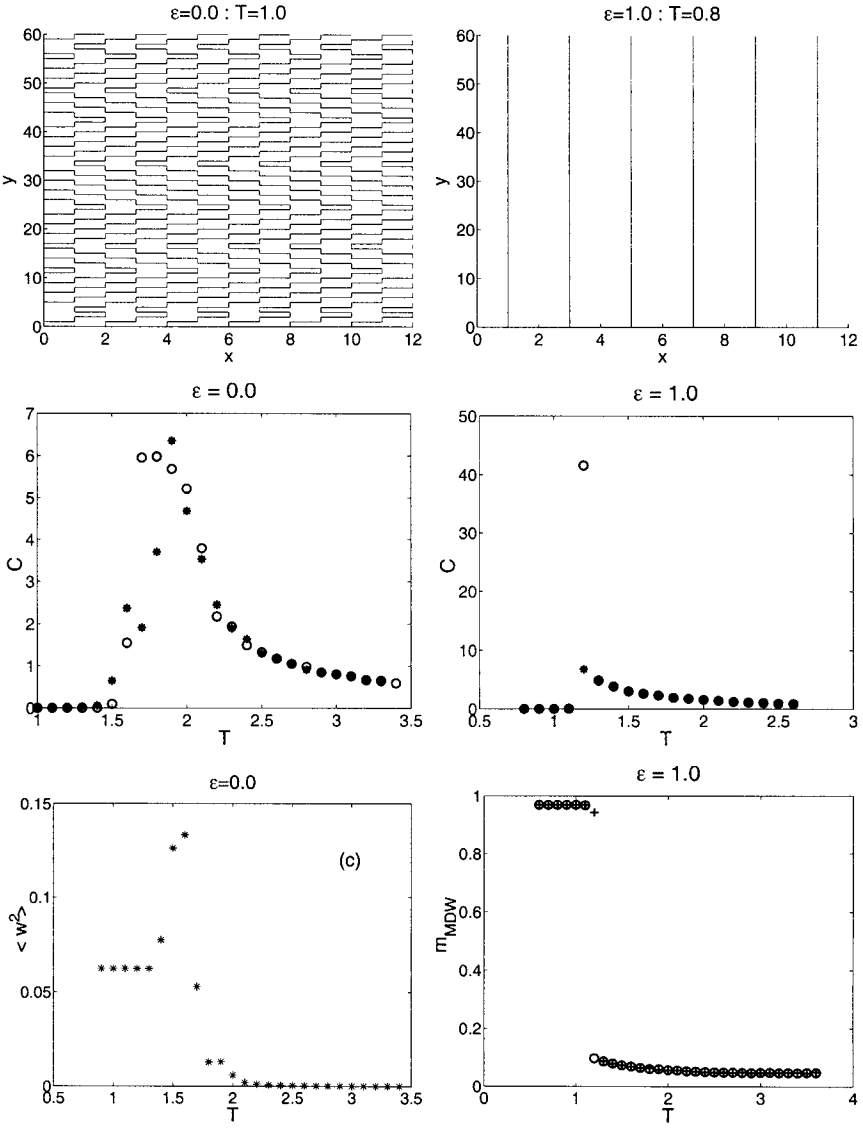

Fig. 4. Representative configurations (top panel) of polymer chains in our model for directed polymers at low temperatures showing the winding phase for $\varepsilon = 0$ (left) and the mass-density-wave phases for $\varepsilon = 1.0$ (right). Plots of the specific heat C (middle panel), and the square of the winding number $\langle W^2 \rangle$ and the mass-density-wave order parameter m_{MDW} (bottom panel) versus temperature T. The transition is continuous for $\varepsilon = 0$ (we believe of the Kosterlitz–Thouless type), but the order parameter shows a jump for $\varepsilon = 1$ (the specific heat is reminiscent of that for KDP type models).

continuous transition of the Kosterlitz–Thouless type as we discuss in detail in ref. 33 (however, metastability problems make it hard to get good-quality data for $\langle W^2 \rangle$ at low T). This is what we would expect from the mapping of our model to models of interacting bosons of one dimension, which show superfluid phases with algebraically decaying correlations. A detailed study of the dependence of $\langle W^2 \rangle$ on L_x and L_y would be interesting to check, in particular, the dependence of finite-size effects on boundary conditions discussed in ref. 69 in the context of bosonic models and flux lines in superconductors. As noted there, free boundary conditions, more appropriate for flux-line and directed-polymer problems than the periodic boundary conditions used for bosonic models, can suppress a sharp phase transition between the disordered and the winding phase. This is because the correspondence between inverse temperature and sample size along the field direction in the flux-line problem is only approximate; we refer the reader to ref. 69 for further details. We also wish to remark here that, if the density of open ends is finite in our system of directed, equilibrium polymers, then the sharp transition between the disordered phase and the winding phase is also suppressed; it is sharp only if there are no open ends. Note also that a Mott-insulating phase arises in bosonic models only because of the underlying pinning potential introduced by the lattice itself; such a phase would not be present in a continuum model without an externally imposed pinning potential.

3.2.3. Continuum Models

As in the lattice-model work of ref. 43–45 we get a disordered isotropic (**I**) phase with low mean lengths $\langle L \rangle$ of self-assembled polymers at high T. This phase transforms into one that is nematically ordered (**N**) at a first-order phase transition as we lower the temperature. Representative configurations in these isotropic and nematic phases of self-assemled polymers are shown in Fig. 5 for our off-lattice model. We expect that these equilibrium polymers will have an exponential distribution of lengths. The distribution $P(L)$ of lengths is shown in a semilog plot versus L for two representative sets of parameter values in Fig. 6 and at temperatures in the vicinity of the isotropic-nematic transition. Note that by the length L we mean the number of monomers in a chain. The distribution does not change significantly with the system size; but care must be exercised in the low-temperature phase as we discuss below while presenting our results for the mean length in the nematic phase.

Figure 7 shows various plots of the internal energy U/ϵ, the nematic order parameter s, and the mean length $\langle L \rangle$ versus the temperature for $\mu/\epsilon = -0.023$, $H_n/\sqrt{\epsilon} = 0.0293$, and $\epsilon/\epsilon_3 = 4.66$. The hysteresis loops in all

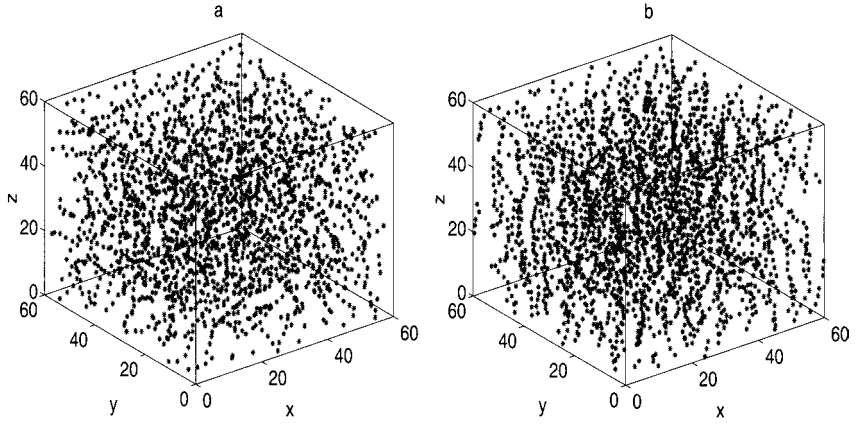

Fig. 5. Representative instantaneous snapshots of monomer configurations in our off-lattice model from our Monte Carlo simulations for $\mu/\epsilon = -0.0223$, nematic-ordering field $H_n/\sqrt{\epsilon} = 0.0293$, and $\epsilon/\epsilon_3 = 4.66$ for (a) a disordered configuration at $T/\epsilon = 0.00757$ and (b) a nematically ordered configuration showing aligned, self-assembled equilibrium polymers at $T/\epsilon = 0.00707$.

the plots of Fig. 7 indicate that the isotropic-nematic transition in our off-lattice model is first-order, just as it is in the lattice model of refs. 43–45 in three dimensions. In these hysteresis loops cooling runs are indicated by full circles •, and heating runs by open circles ◦. The widths of these hysteresis loops depend of course on cooling and heating rates; if the system is cooled infinitely slowly, these loops will be replaced by equilibrium jump discontinuities in U/ϵ, s, and $\langle L \rangle$ at the first order transition. We have investigated the dependence of hysteresis loops on the linear size ℓ of our

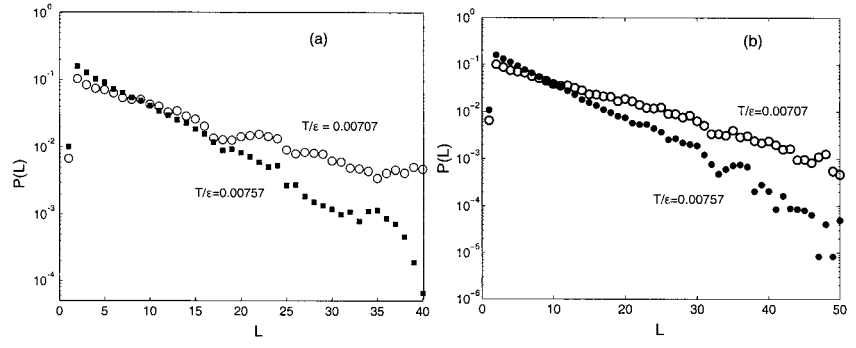

Fig. 6. Semilog plot of the length distribution $P(L)$ of polymers of length L in the vicinity of the isotropic-nematic transition (at $T/\epsilon = 0.00757$ and $T/\epsilon = 0.00707$ for the parameters used here). $P(L)$ can be fit to an exponential form for $2L\sigma < \ell$, where ℓ is the length of the cubical simulation box. $\epsilon/\epsilon_3 = 4.66$, $\mu/\epsilon = -0.0223$, $H_n/\sqrt{\epsilon} = 0.0293$, and (a) $\ell = 60\sigma$ and (b) $\ell = 78\sigma$.

cubical simulation box and cooling and heating rates. Figures 7(a)–(c) are obtained with $\ell = 60\sigma$ and a temperature difference of $\Delta T/\epsilon = 7.14 \times 10^{-5}$ between successive temperatures in our heating and cooling scans. Figures 7(d)–(f) are analogous plots for a larger system size, $\ell = 78\sigma$, with all other parameters as in Figs. 7(a)–(c). In Figs. 7(g)–(i), all parameters are as in Figs. 7(a)–(c) except for the cooling and heating rates which are halved with $\Delta T/\epsilon = 3.57 \times 10^{-5}$. A comparison of the top, middle and

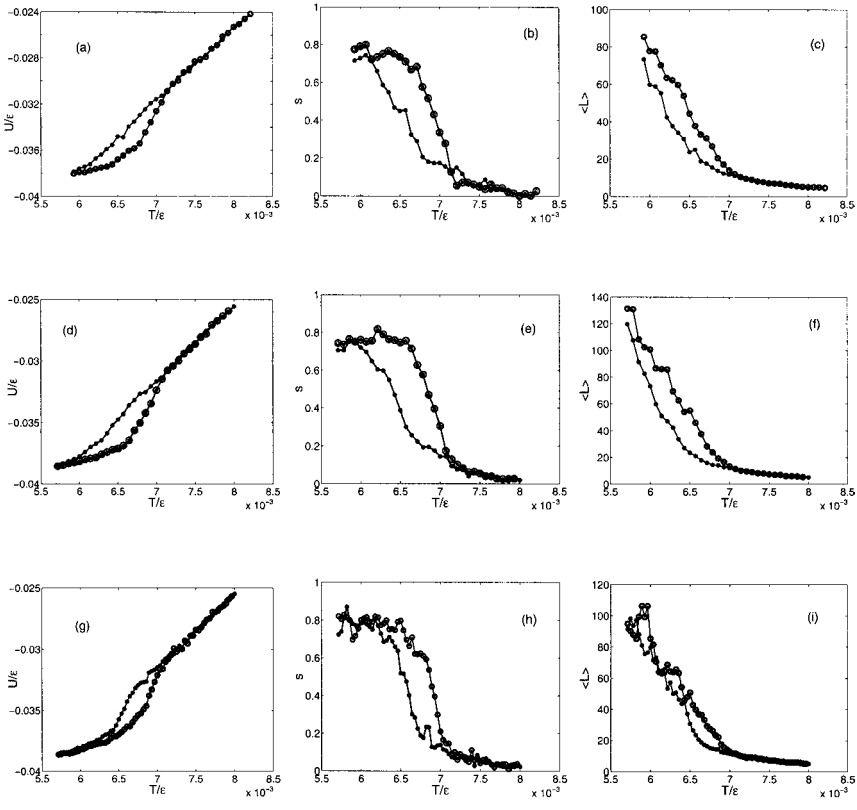

Fig. 7. Plots of the energy U/ϵ, the nematic order parameter s, and the mean length $\langle L \rangle$ versus temperature T for $\mu/\epsilon = -0.023$, $\epsilon/\epsilon_3 = 4.66$ and $H_n/\sqrt{\epsilon} = 0.0293$ showing hysteresis loops. The jumps at the transition temperature broaden into a hysteresis loop because our temperature scan through the transitions is not slow enough relative to the equilibration times in our system: (a–c) Data for a cubical simulation box of size with side $\ell = 60\sigma$, and a cooling and heating rate that corresponds to a temperature difference of $\Delta T/\epsilon = 7.14 \times 10^{-5}$ between successive points; (c–f) data for a cubical simulation box of size with side $\ell = 78\sigma$ and the same heating and cooling rate; (g–i) data for a cubical simulation box of size with side $\ell = 60\sigma$ but the cooling and heating rate halved to $\Delta T/\epsilon = 3.57 \times 10^{-5}$. Full circles • represent the cooling runs whereas open circles ∘ represent the heating runs.

bottom panels of Fig. 7 indicate, therefore, that U/ϵ and s do not have a significant size dependence since the data for $\ell = 60\sigma$ and $\ell = 78\sigma$ are comparable; also the widths of the hysteresis loops decrease as we decrease cooling and heating rates, which is in accordance with our general expectations. Note that, away from the isotropic-nematic transition, our cooling and heating runs coincide indicating that our data are well equilibrated.

The value of $\langle L \rangle$ is independent of ℓ ($\geqslant 60\sigma$) in the high-temperature isotropic phase; however, in the low-T nematic phase $\langle L \rangle$ increases substantially as ℓ goes from 60σ to 78σ; indeed, many polymers loop around our simulation box because of the periodic boundary conditions we use. Only much larger simulations than those reported here can settle whether $\langle L \rangle \sim \ell$ in the low-T nematic phase, or whether, eventually, $\langle L \rangle$ saturates to a temperature dependent but ℓ-independent value for all temperatures below the ordering temperature. At $T = 0$ this value of $\langle L \rangle$ could then diverge with ℓ, but other phases like the hexagonal columnar phase could also form at lower values of T than explored here.

We have checked explicitly that no branching of polymers occurs in our model. For example, consider the case $\epsilon/\epsilon_3 = 1.4$, $\mu/\epsilon \simeq -0.0171$, and $H_n/\sqrt{\epsilon} \simeq 0.0207$: if $T/\epsilon \simeq 0.0071$, which lies above the isotropic-nematic transition temperature, there are on average 2009 monomers and 358 chains (including single-monomer and dimer units); at $T/\epsilon \simeq 0.00543$, which lies below the isotropic-nematic transition temperature, there are on average 3262 monomers and 29 chains. In both these cases there are no monomers with more than two other monomers as neighbours; i.e., there is no branching of polymers that self-assemble in our model.

We have also obtained thermodynamic functions at a higher value of ϵ_3 (than in Fig. 7). Representative results for $\epsilon/\epsilon_3 = 1.4$ are shown in Fig. 8. A comparison of the hysteresis loops in Fig. 8 with those in Fig. 7 ($\epsilon/\epsilon_3 = 4.66$) indicates that, as ϵ_3 increases, so does the latent heat at the isotropic-nematic transition. (Of course we must exercise some caution while estimating latent heats from the wide hysteresis loops of Figs. 7 and 8.) The data of Fig. 8 show that the hysteresis loops become narrower as we increase $H_n/\sqrt{\epsilon}$; also the nematic phase forms at a higher temperature as is to be expected. Figures 9(a) and (b) show, respectively, plots of the mean aspect ratio A of the polymers and the number N of monomers in our simulation box as functions of T/ϵ for $\epsilon/\epsilon_3 = 4.66$ (full lines) and $\epsilon/\epsilon_3 = 1.4$ (dashed lines), $\mu/\epsilon = -0.023$, $\ell = 60\sigma$, and $H_n/\sqrt{\epsilon} = 0.0293$. Since A increases clearly with increasing ϵ_3 [Fig. 9(a)] it is tempting to interpret ϵ_3 as a parameter whose principal role is to make the polymers semiflexible. However, a careful consideration of our potentials [Eqs. (1)–(2)] shows that a change in ϵ_3 also changes other properties of our potentials, such as the depth of the curves shown in Fig. 3 at fixed values of θ. Figure 9(b)

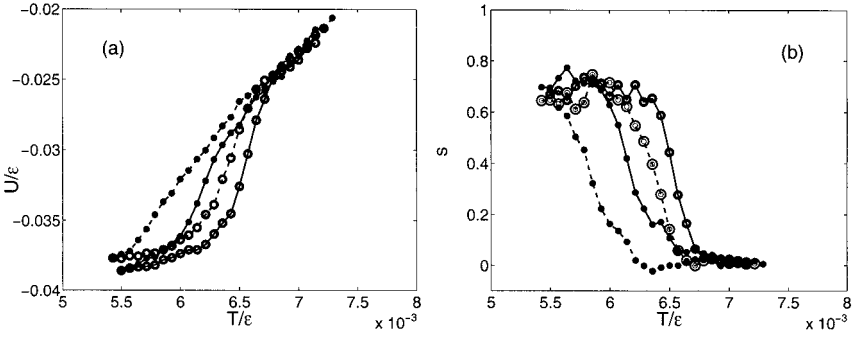

Fig. 8. Plots of (a) energy U/ϵ and (b) nematic order parameter s versus T/ϵ for our off-lattice model with $\epsilon/\epsilon_3 = 1.4$ and $\mu/\epsilon = -0.023$ for a cubical box of size $\ell = 60\sigma$. Dashed lines joining data points indicate $H_n/\sqrt{\epsilon} = 0.0207$ whereas full lines indicate $H_n/\sqrt{\epsilon} = 0.0293$. Full circles • represent cooling runs whereas open circles ◦ represent heating runs. As $H_n/\sqrt{\epsilon}$ increases, the nematic phase forms at a higher temperature as expected.

shows the range of values of the number of monomers N in the vicinity of the isotropic-nematic transition.

The measurements of the thermodynamic functions shown in Figs. 7–9 can be used to obtain the phase diagram for our off-lattice model. Two representative phase diagrams are shown in Fig. 10 in the μ–T plane for different parameter values. These phase diagrams show the isotropic and nematic phases separated by a first-order phase boundary (dashed line). The error bars on these phase boundaries are large since the hysteresis loops [Figs. 7–9] are quite wide given our cooling and heating rates. These

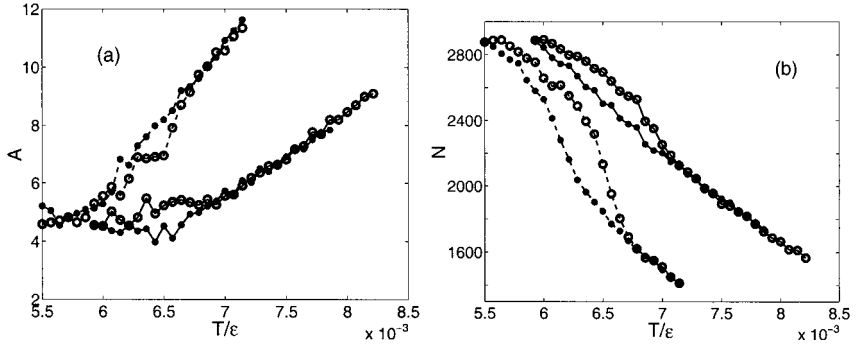

Fig. 9. Plots of (a) the average aspect ratio A and (b) the total number of monomers N versus temperature T for our off-lattice model with $\epsilon/\epsilon_3 = 4.66$ (full lines between data points) and $\epsilon/\epsilon_3 = 1.4$ (dashed lines) for $\mu/\epsilon = -0.023$, $H_n/\sqrt{\epsilon} = 0.0293$, and a cubical box of size $\ell = 60\sigma$. Full circles • represent cooling runs whereas open circles ◦ represent heating runs.

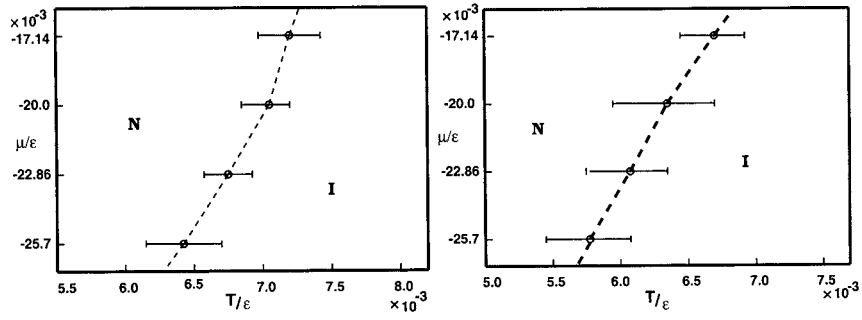

Fig. 10. Phase diagrams in the μ–T plane showing the first-order phase boundary separating the isotropic (I) and nematic (N) phases for $\epsilon/\epsilon_3 = 4.66$, $H_n/\sqrt{\epsilon} = -0.0293$ (left panel) and $\epsilon/\epsilon_3 = 1.4$ and $H_n/\sqrt{\epsilon} = -0.0207$ (right panel) for our off-lattice model. The large error bars in the transition temperature correspond to the widths of the order parameter hysteresis loops in Fig. 7.

error bars are estimated by the difference in temperature between the heating and cooling runs at the point at which the order parameter $s = 0.4$, which occurs roughly in the middle of the hysteresis loop.

We have shown previously[32] that our model of semiflexible polymers shows shear alignment. When we apply shear by the dynamic Monte Carlo method described above, the self-assembled polymers in our off-lattice model get nematically aligned and the system exhibits a positive value of s at temperatures that are too high for the formation of a nematic phase in the absence of shear. Thus shear promotes nematic ordering at low shear rates. However, higher shear rates reduce this nematic alignment by tearing

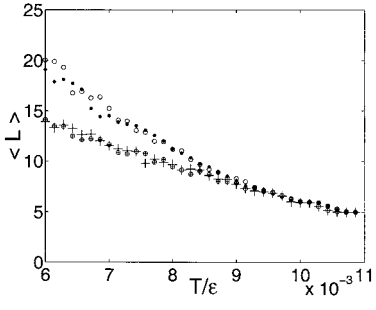

Fig. 11. The variation of the mean length of polymers $\langle L \rangle$ with T/ϵ for $\mu/\epsilon = -0.0214$, $H_n/\sqrt{\epsilon} = 0$ and with an imposed shear. The strength of the shear is measured by the parameter B defined in the text. For $B = 0.00018$, cooling runs are indicated by $(+)$ and heating runs by $\oplus$; and for $B = 0.00007$, cooling runs are indicated by $\bullet$ and heating runs by open circles $\circ$.

apart the chains of equlibrium polymers. This is illustrated in the plot of the mean length $\langle L \rangle$ versus temperature (Fig. 11) for two different shear rates. However, hydrodynamic effects are not incorporated in the dynamic Monte Carlo method we use to apply shear. This dynamic Monte Carlo method is, therefore, not suitable for studies of the rheological properties of our off-lattice model and cannot, in particular, be used to study the shear banding we expect in these systems;[9, 10] these must await equilibrium-polymer analogs of the Molecular Dynamics simulations[47] used for systems of semiflexible polymers.

We have described above the cooling and heating protocols that we use in our scanning calorimetry studies of glasses in our off-lattice model. Our results for these are illustrated in the plots of Fig. 12 for $\mu/\epsilon = -0.023$, $\epsilon/\epsilon_3 = 1.4$, and $H_n/\sqrt{\epsilon} = 0.0207$. The cooling runs are carried out at a rate

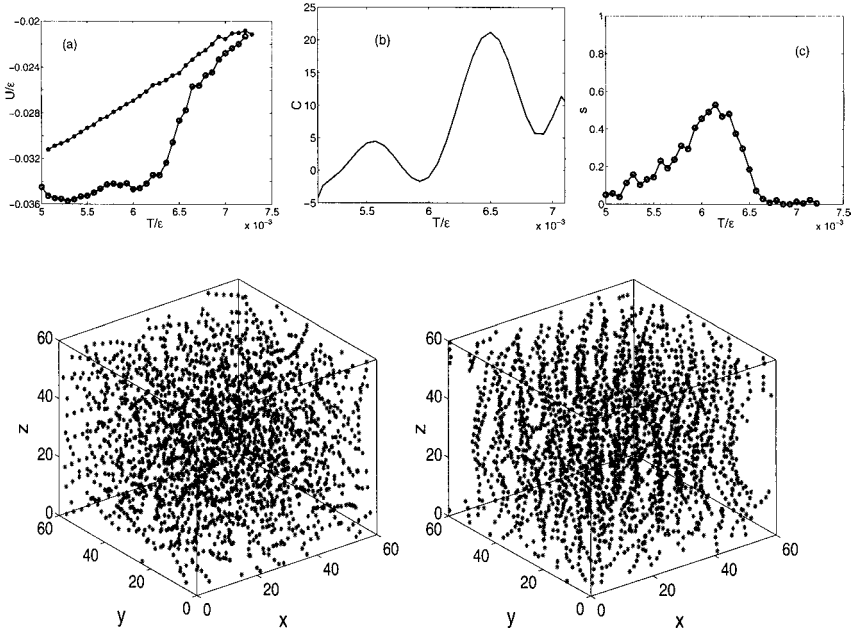

Fig. 12. Scanning-calorimetry plots for our off-lattice model showing (a) U/ϵ, (b) the derivative, with respect to T, of a polynomial fit to U/ϵ (heating run), and (c) the nematic order parameter s for $\mu/\epsilon = -0.023$, $\epsilon/\epsilon_3 = 1.4$ and $H_n/\sqrt{\epsilon} = 0.0207$ for a system of size $60\sigma \times 60\sigma \times 60\sigma$ with periodic boundary conditions. The rapid-cooling scan is indicated by • and the heating runs by open circles (∘). The dip in C just before $T/\epsilon \simeq 0.006$ in (b) corresponds to the transition from a low temperature glass, formed on rapid cooling, to the nematic phase. The plotted configurations are at the lowest temperature immediately after rapid cooling (left) and at the temperature which shows the highest nematic order on heating (right).

that is fast enough to prevent equilibration; instead a disordered, metastable, glassy state obtains as shown in the representative configuration of entangled, self-assembled polymers on the bottom left of Fig. 12. Slow heating along the heating part of our scanning calorimetry curves makes this disordered configuration evolve into one with a fair degree of nematic order; a representative configuration with such nematic order is shown on the bottom right of Fig. 12. Figure 12(a) shows the variation of the internal energy U/ϵ versus temperature for both the rapid-cooling and the slow-heating scans. A derivative, with respect to T, of the heating scan yields the differential-scanning-calorimetry (DSC) plot of the "specific heat" C versus the temperature shown in Fig. 12(b). The first dip in this specific heat marks the temperature where the glassy configuration changes to the low-T equilibrium phase (a nematic here). The subsequent peak indicates the change from the low-T equilibrium phase to the high-T (isotropic) phase.

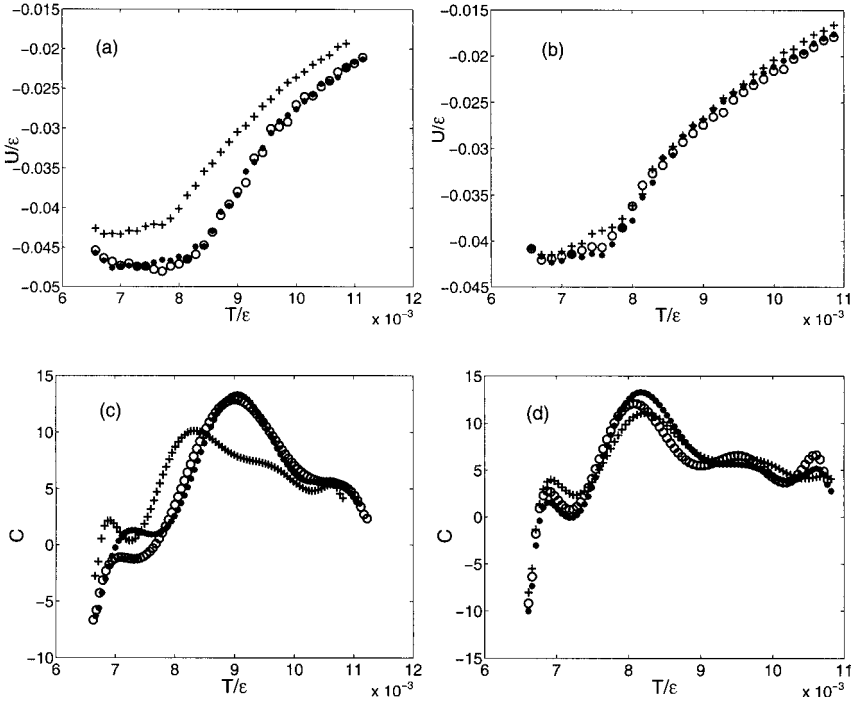

Fig. 13. Scanning calorimetry plots, as in Figs. 12(a) and (b) but for a system with attractive walls [(a) and (c)] and neutral walls [(b) and (d)], showing U/ϵ [(a) and (b)] and $C = dU/dT$ [(c) and (d)] versus temperature T/ϵ. Periodic boundary conditions are used in the y and z directions with a box of length of 60σ. The walls normal to the x direction are separated by 18σ (*), 36σ($\circ$) and 72σ (+). A 9-th order polynomial was fitted to the data of (a) and (b) and the derivative of this polynomial was used to obtain $C = dU/dT$ for (c) and (d).

To make contact with experiments, we plot C (i.e., dU/dT) versus T. This differential-scanning plot is qualitatively similar to ones obtained in experimental polymeric glasses. Also, our results here are akin to those for the lattice model of refs. 43–45. Figure 12(c) shows how the nematic order parameter rises from near zero, in the glassy state, to about 0.6 in the heating run here before it falls to zero again in the equilibrium, isotropic phase at high T/ϵ.

We have also carried out scanning-calorimetry studies of our off-lattice models in the presence of attractive and neutral walls. These results are given in the plots of Fig. 13. Our study here has been motivated by the recent interest[70] in the dependence of the glass transition temprature in polymeric glasses on the properties of walls in narrow, confining systems. Given our off-lattice model, it is easy for us to repeat our scanning-calorimetry procedure with attractive or neutral walls separated by different distances. We do not directly determine a glass transition in our studies, but we can certainly identify the first minimum in our DSC scans, which is

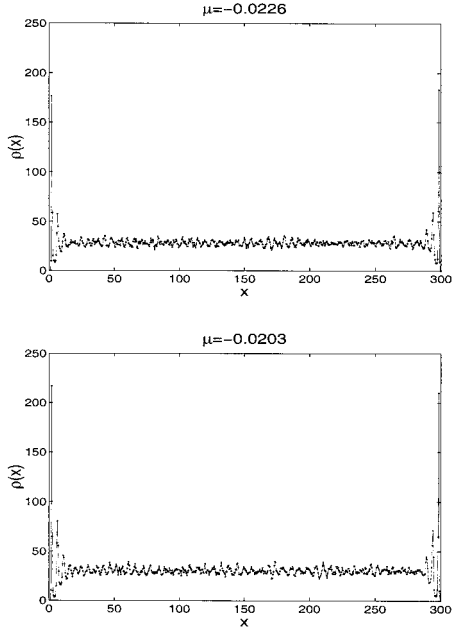

Fig. 14. The layer number of monomers $\rho(x)$ in a slice of width $\sigma \times 60\sigma \times 60\sigma$ versus x, the normal distance from the wall at $x = 0$, showing the adsorption of semiflexible, equilibrium polymers in our model at attractive walls placed at $x = 0$ and $x = 300\sigma$. Data have been obtained in the vicinity of the bulk isotropic-nematic transition for $(\epsilon/\epsilon_3 = 1.4)$ and $T/\epsilon \simeq 0.0066$ for two different values of the chemical potential.

associated with the conversion of the glass into a nematically ordered state. The position of this minimum is clearly visible in the plots of Fig. 13 for different wall separations and the cases of attractive walls (left panels) and neutral walls (right panels). As we might expect, attractive walls have a more dramatic effect on the position of this minimum. In Fig. 14 we show for comparison how attractive walls lead to the adsorption of monomers, in equilibrium, in our off-lattice modeli; such adsorption leads to an increased density near the walls and, in equilibrium, an attendant enhancement of the nematic order parameter there.

4. CONCLUSIONS

Our aim in this paper has been to give an overview of the salient points in the statistical mechanics of semiflexible, equilibrium polymers and related systems of living polymers. These comprise a large class of systems, including soultions of wormlike micelles or poly(α methylstyrene). The polymers attain an equilibrium length distribution $P(L)$, which has typically an exponential form (power-law prefactors modify the exponential in the dilute limit). If the collection of self-assembled polymers is dense enough and semiflexibility induces the formation of elongated chains, then interactions precipitate the formation of a polymer-nematic phase as the temperature is lowered. The polymers align if such systems are sheared; and the formation of a nematic phase is preempted by glass formation if the cooling rate is not slow enough. Furthermore, there has been a recent suggestion[59] that one can obtain physical realizations of directed, semiflexible, equilibrium.

We have tried to study these phenomena, especially those associated with the formation of nematic phases or glassy states, by using both lattice and off-lattice models. There have been other studies, some using lattice models and others with continuum models, of different aspects of the statistical mechanics of this class of systems; we have summarized these above. However, we are not aware of any other work that integrates the study of equilibrium phases, directed equilibrium polymers, glass formation, surface adsorption, and shear alignment in these systems by using related lattice and continuum models. We have attempted this here in the hope that the collection of these studies in one place will stimulate new experimental studies of this fascinating class of polymeric systems.

We have discussed our results above; further details can be found in refs. 32, 33, and 43–45. Here we highlight those aspects of our results that we hope will lead to novel experiments. It would be extremely interesting to see if the polymer analogs of the superfluid and mass-density-wave phases mentioned above can be obtained in the experimental realizations of

directed, equilibrium polymers mentioned in ref. 59. Equilibrium phase diagrams, say density-temperature versions of the ones shown in Fig. 10, would be very welcome, especially if they could be studied as a function of the chain stiffness. Shear-alignment and shear-banding experiments are perhaps ahead of simulations here; molecular-dynamics simulations of shear banding in models for equilibrium, semiflexible polymers are certainly worth undertaking. So too are experimental differential-scanning-calorimetry studies of glassy states in these systmes, whose Monte Carlo analogs we have discussed in detail above. And last, experimental studies of the adsorption of semiflexible, equilibrium polymers are well worth carrying out along the lines of our illustrative Monte Carlo studies of these issues.

ACKNOWLEDGMENTS

We thank Chinmay Das, Gautam Menon, and Sriram Ramaswamy for useful discussions and SERC (IISc) for computational facilities.

REFERENCES

1. M. E. Cates, *J. Phys. Condens. Mat.* **8**:9167 (1996).
2. H. Rehage and H. Hoffman, *Mol. Phys.* **74**:933 (1991).
3. L. Magid, *J. Phys. Chem. B* **102**:4064 (1998).
4. S. V. G. Menon, P. S. Goyal, B. A. Dasanacharya, S. K. Paranjpe, R. V. Mehta, and R. V. Upadhyay, *Physica B* **213**:604 (1996).
5. J. Santhanalakshmi, G. Shanthanalaksmi, V. K. Aswal, and P. S. Goyal, *Proc. Indian Acad. Sci. (Chem Sci.)* **113**:55 (2001).
6. J. Narayanan, C. Manohar, and E. Mendes, *J. Chem. Phys.* **100**:18524 (1996).
7. J. Narayanan, W. Urbach, D. Langevin, C. Manohar, and R. Zana, *Phys. Rev. Lett.* **81**:228 (1998); J. Naranayanan, C. Manohar, D. Langevin, and W. Urbach, *Langmuir* **13**:398 (1997).
8. R. Oda, J. Narayanan, P. A. Hassan, C. Manohar, R. A. Salkar, F. Kern, and S. J. Candau, *Langmuir* **14**:4364 (1998).
9. A. K. Sood, R. Bandyopadhyay, and G. Basappa, *Pramana, J. Physics* **53**:223 (1999).
10. R. Badyopadhyay, G. Basappa, and A. K. Sood, *Phys. Rev. Lett.* **84**:2022 (2000).
11. R. L. Scott, *J. Phys. Chem.* **69**:261 (1965); R. F. Bacon and R. Fanelli, *J. Amer. Chem. Soc.* **65**:639 (1943).
12. F. Livolani and Y. Boulingad, *J. Phys. (Paris)* **47**:1813 (1986); R. Podgornik, D. C. Rau, and V. A. Parsegian, *Macromolecules* **22**:1780 (1989).
13. K. M. Zheng and S. C. Greer, *Macromolecules* **25**:6128 (1992).
14. K. M. Zheng, S. C. Greer, L. Rene Corrales, and J. Ruiz Garcia, *J. Chem Phys.* **98**:9873 (1993).
15. A. P. Andrews, K. P. Andrews, S. C. Greer, F. Boue, and P. Pfeuty, *Macromolecules* **27**:3902 (1994).
16. S. Sarkar Das, A. P. Andrews, and S. C. Greer, *J. Chem. Phys.* **102**:2951(1995).
17. J. Zhuang, A. P. Andrews, and S. C. Greer, *J. Chem. Phys.* **107**:4705 (1997).
18. A. V. Tobolsky and A. Eisenberg, *J. Colloid Sci.* **17**:49 (1962).

19. J. C. Wheeler, S. J. Kennedy, and P. Pfeuty, *Phys. Rev. Lett.*, **45**:1748 (1980); J. C. Wheeler, S. J. Kennedy, and P. Pfeuty, *J. Chem. Phys.* **78**:954 (1983).
20. J. Ruiz-Garcia, Ph.D. dissertation (University of Maryland, College Park, 1989).
21. J.-F. Berret, D. C. Roux, G. Porte, and P. Lindner, *Europhys. Lett.* **32**:137 (1995).
22. E. Fischer and P. T. Callaghan, *Phys. Rev. E* **64**:11501 (2001).
23. H. Rehage and H. J. Hoffman, *J. Phys. Chem.* **92**:4712 (1988).
24. J. F. Berret, *Langmuir* **13**:2227 (1997).
25. P. A. Hassan, B. S. Valaulikar, C. Manohar, F. Kern, L. Bourdieu, and S. J. Candau, *Langmuir* **18**:4350 (1996).
26. M. E. Cates and S. J. Candau, *J. Phys. Condens. Mat.* **2**:6869 (1990).
27. P. Mukerjee, *J. Phys. Chem.* **76**:565 (1972).
28. M. E. Cates, *Macromolecules* **20**:2289 (1987).
29. J. P. Wittmer, A. Milchev, and M. E. Cates, *J. Chem. Phys.* **109**:834 (1998).
30. P. van der Schoot, *J. Chem Phys.* **104**:1130 1996.
31. P. van der Schoot and M. E. Cates, *Europhys. Lett.* **25**:515 (1994).
32. A. Chatterji and R. Pandit, *Europhys. Lett.* **54**:213(2001).
33. A. Chatterji and R. Pandit, To be submitted, (2002).
34. J. P. Wittmer, A. Milchev, and M. E. Cates, *Europhys. Lett.* **41**:291 (1998).
35. A. Milchev, W. Paul, and K. Binder, *J. Chem. Phys.* **99**:4786 (1993).
36. A. Milchev, J. P. Wittmer, and D. P. Landau, *Euro. Phys. J. B* **12**:241 (1999).
37. A. Milchev, J. P. Wittmer, and D. P. Landau, *Phys. Rev. E* **61**:2959 (2000).
38. I. Carmesin and K. Kremer, *Macromolecules* **21**:2819 (1998).
39. Y. Rouault, *J. Phys. II France* **6**:1301 (1996).
40. Y. Rouault and A. Milchev, *Europhys. Lett.* **33**:341 (1996).
41. G. F. Tuthill and M. V. Jaric, *Phys. Rev. B* **31**:5 (1985); G. F. Tuthill and M. V. Jaric, *Phys. Rev. B* **31**:2981 (1985).
42. A. Milchev and D. P. Landau, *Phys. Rev. E* **52**:6431 (1995).
43. G. I. Menon, R. Pandit, and M. Barma, *Europhys. Lett.* **24**:253 (1993).
44. G. I. Menon and R. Pandit, *Phys. Rev. Lett.* **75**:4638 (1995).
45. G. I. Menon and R. Pandit, *Phys. Rev. E* **59**:787 (1999).
46. I. Geroff, A. Milchev, K. Binder, and W. Paul, *J. Chem. Phys.* **98**:6526 (1993).
47. F. Affouard, M. Kroger, and S. Hess, *Phys. Rev. E* **54**:5178 (1996).
48. Y. Rouault, *J. Chem. Phys.* **111**:9859 (1999).
49. M. Dijkstra and D. Frenkel, *Phys. Rev. E* **51**:5891 (1995).
50. A. Milchev, Y. Rouault, and D. P. Landau, *Phys. Rev. E* **56**:1946 (1997).
51. R. D. Kamien and G. S. Grest, *Phys. Rev. E* **55**:1197 (1997).
52. S. J. Kennedy and J. C. Wheeler, *J. Chem Phys* **78**:953 (1983).
53. J. C. Wheeler, *Phys. Rev. Lett.* **53**:174 (1984); J. C. Wheeler, *J. Chem Phys* **81**:3635 (1984).
54. S. J. Kennedy and J. C. Wheeler, *J. Chem. Phys.* **78**:1523 (1983).
55. R. Petschek, P. Pfeuty, and J. C. Wheeler, *Phys. Rev. A* **34**:2391 (1986); J. P. Wittmer, P. van der Schoot, A. Milchev, and J. L. Barrat, *J. Chem. Phys.* **113**:6992 (2000); A. Milchev, J. P. Wittmer, P. van der Schoot, and D. Landau, *Europhys. Lett.* **54**:58 (2001).
56. P. J. Flory, *Proc. R. Soc. London, Ser A* **234**:60 (1956); **234**:73 (1956).
57. A. Baumgartner, *J. Phys. A* **17**:L971 (1984); A. Baumgartner, *J. Chem. Phys.* **84**:13 (1986); A. Baumgartner and D. Y. Yoon, *J. Chem. Phys.* **79**:521 (1983).
58. P. D. Gujrati and M. Goldstein, *J. Chem. Phys.* **74**:2596 (1981).
59. S. Jain and D. R. Nelson, *Phys. Rev. E* **61**:1599 (2000).
60. T. D. Kuhner, S. R. White, and H. Monien, *Phys. Rev. B* **61**:12474 (2000); T. D. Kuhner and H. Monien, *Phys. Rev. B* **58**:14741 (1998); R. V. Pai and R. Pandit, to be published.

61. D. R. Nelson and H. S. Seung, *Phys. Rev. B* **39**:9153 (1989).
62. R. D. Kamien, P. Le Doussal, and D. R. Nelson, *Phys. Rev. A* **45**:8727 (1992).
63. D. M. Ceperley and E. L. Pollock, *Phys. Rev. B* **30**:2555 (1984); W. Krauth and N. Trivedi, *Europhys. Lett.* **14**:627 (1991); D. M. Ceperley, *Rev. Mod. Phys.* **67** (1995).
64. W. Krauth, N. Trivedi, and D. Ceperley, *Phys. Rev. Lett.* **67**:2307 (1991).
65. D. R. Nelson and A. Stern, *Proceedings XIV Sitges Conference, Complex Behavior of Glassy Systems, June 10–14 (1996)*, N. Rubi, ed., cond-mat 9701001.
66. E. H. Lieb and F. Y. Wu, in *Phase Transitions and Critical Phenomena*, Vol. 1, C. Domb and M. S. Green, eds. (Academic Press, New York, 1972), pp. 331–490.
67. R. Pandit, M. Schick, and M. Wortis, *Phys. Rev. B* **26**:5112 (1982).
68. If the monomers interact with a substrate via a Lennard–Jones potential, then a lateral average over a semi-infinite, planar substrate yields a monomer-substrate potential of the form given in Eq. (3). See, e.g., R. Pandit in *Recent Advances in Theoretical Physics*, R. Ramachandran, ed. (World Scientific, Singapore, 1985), pp. 302–342; M. Wortis, R. Pandit, and M. Schick, in *Melting Localization and Chaos*, R. K. Kalia and P. Vashishta, eds. (North-Holland, New York, 1982), pp. 13–27; C. Ebner and W. F. Saam, *Phys. Rev. Lett.* **38**:1486 (1977).
69. U. C. Tauber and D. R. Nelson, *Phys. Rep.* **289**:157 (1997).
70. P. G. de Gennes, *Eur. Phys. J. E* **2**:201 (2000); K. Binder, *Eur. Phys. J. E* **2**:204 (2000); R. A. L. Jones, *Eur. Phys. J. E* **2**:205 (2000).